

THESIS FOR THE DEGREE OF LICENTIATE OF ENGINEERING

Turbulent impurity transport in tokamak fusion plasmas

Andreas Skyman



CHALMERS

Department of Earth and Space Sciences
CHALMERS UNIVERSITY OF TECHNOLOGY
Göteborg, Sweden 2011

Turbulent impurity transport in tokamak fusion plasmas
ANDREAS SKYMAN

© ANDREAS SKYMAN, 2011

Technical Report 49L

Department of Earth and Space Sciences
Chalmers University of Technology
SE-412 96 Göteborg, Sweden
Phone: +46 (0)31-772 1000

Printed in Sweden
Chalmers Reproservice
Göteborg, Sweden 2011

Contact information:

Andreas Skyman
Department of Earth and Space Sciences
Chalmers University of Technology
Hörsalsvägen 9
SE-412 96i Göteborg, Sweden

Phone: +46 (0)31-772 1715

Fax: +46 (0)31-772 3663

Email:  andreas.skyman@chalmers.se

URL:  <http://www.dd.chalmers.se/~skymandr>

Last updated on December 21, 2011.

An up to date version of this thesis will be available on the author's homepage.



This work is licensed under the *Creative Commons Attribution-ShareAlike 3.0 License*.

The license text may be obtained at

 <http://creativecommons.org/licenses/by-sa/3.0/>

or by writing to

Creative Commons
Squad 171 Second St, Suite 300
San Francisco, CA 94105 USA

Typeset in L^AT_EX using free open source software.

Turbulent impurity transport in tokamak fusion plasmas

Andreas Skyman

*Transport Theory, Department of Earth and Space Sciences
Chalmers University of Technology*

Thesis for the degree of Licentiate of Engineering
a Swedish degree between M.Sc. and Ph.D.

Abstract

With the enormous growth of high performance computing (HPC) over the last few decades, plasma physicists have gained access to a valuable instrument for investigating turbulent plasma behaviour. In this thesis, these tools are utilised for the study of particle transport in fusion devices of the tokamak variety, focusing in particular on the transport of impurities.

The transport properties of impurities is of high relevance for the performance and optimisation of magnetic fusion devices. For instance, the possible accumulation of He ash in the core of the reactor plasma will serve to dilute the fuel, thus lowering fusion power. Heavier impurity species, originating from the plasma-facing surfaces, may also accumulate in the core, and wall-impurities of relatively low density may lead to unacceptable energy losses in the form of radiation. In an operational power plant, such as the ITER device, both impurities of low and high charge numbers will be present.

This thesis studies turbulent impurity transport driven by two different modes of drift wave turbulence: the trapped electron (TE) and ion temperature gradient (ITG) modes. Principal focus is on the balance of convective and diffusive impurity transport, as quantified by the impurity density gradient of zero flux (“peaking factor”, PF). The results are scalings of PF with impurity charge number, as well as with the driving background gradients of temperature and density, as well as other plasma parameters.

Quasi- and nonlinear results are obtained using the gyrokinetic code GENE, and compared with results from a computationally efficient multi-fluid model. In general, the three models show a good qualitative agreement. Results for ITG mode driven impurity transport are also compared with experimental results from the Joint European Torus, and also in this case a good qualitative agreement is obtained.

Keywords: fusion plasma physics, tokamaks, gyrokinetic theory, fluid theory, turbulence, impurity transport, ion temperature gradient mode, trapped electron mode, Joint European Torus, e-science

List of Appended Papers

This thesis is a summary of the following three papers. References to the papers will be made using roman numerals.

Paper I – H. Nordman, **A. Skyman**, P. Strand, C. Giroud, F. Jenko, F. Merz, V. Naulin, T. Tala and the JET–EFDA Contributors,
Fluid and gyrokinetic simulations of impurity transport at JET,
Plasma Physics and Controlled Fusion, vol. 53, no. 10, p. 105005–18

Paper II – **A. Skyman**, H. Nordman, P. Strand,
Impurity transport in temperature gradient driven turbulence,
Physics of Plasmas, (submitted)

Paper III – **A. Skyman**, H. Nordman, P. I. Strand,
Particle transport in density gradient driven TE mode turbulence,
Nuclear Fusion SPE 2012, (submitted)

Other contributions (not included)

This is a list of conference contributions and non-peer reviewed articles.

- A – **A. Skyman**, H. Nordman, P. Strand, et al,
Impurity transport in ITG and TE mode dominated turbulence,
Proceedings of EPS 2010, Europhysics Conference Abstracts, vol. 34A,
<http://ocs.ciemat.es/EPS2010PAP/pdf/P1.1092.pdf>

- B – H. Nordman, **A. Skyman**, P. Strand, et al,
Modelling of impurity transport experiments at the Joint European Torus,
Proceedings of EPS 2010, Europhysics Conference Abstracts, vol. 34A,
<http://ocs.ciemat.es/EPS2010PAP/pdf/P1.1074.pdf>

- C – **A. Skyman**, H. Nordman, P. Strand, et al,
Impurity transport in ITG and TE mode dominated turbulence,
EPS Conference 2010, (poster), Dublin, Ireland
http://publications.lib.chalmers.se/records/fulltext/local_126484.pdf

- D – P. Strand, **A. Skyman**, H. Nordman,
Core transport studies in fusion devices,
SNIC progress report 08/09,
http://publications.lib.chalmers.se/records/fulltext/local_126485.pdf

- E – P. Strand, **A. Skyman**, H. Nordman,
Core transport studies in fusion devices,
PDC 20th Anniversary & SNIC Interaction Conference 2010, (poster), Stockholm, Sweden
http://publications.lib.chalmers.se/records/fulltext/local_126486.pdf

- F – **A. Skyman**, H. Nordman, P. Strand,
Turbulent impurity transport in fusion plasmas,
RUSA meeting 2010, (poster), Stockholm, Sweden
http://publications.lib.chalmers.se/records/fulltext/local_131418.pdf

- G – **A. Skyman**, P. Strand, H. Nordman,
Turbulence and transport in multi ion species fusion plasmas,
PDC Newsletter, vol. 11, no. 1, p. 12,
<http://www.pdc.kth.se/publications/pdc-newsletter/2011-1>

- H – **A. Skyman**, P. Strand, H. Nordman,
Turbulent impurity transport driven by temperature and density gradients,
13th International Workshop on H-mode Physics and Transport Barriers, (poster), Oxford, UK
http://publications.lib.chalmers.se/records/fulltext/local_147191.pdf

Acknowledgements

I would like to express my sincere gratitude to my friends in Hederligheten & Assoc., without whose continuous (and firm, sometimes almost to a fault) support the writing of this thesis would not have been possible (or at least not enjoyable).

I would also like to thank my co-workers, and in particular my supervisor Prof H. Nordman, for rewarding discussions on the finer points of plasma turbulence.¹

Further, I wish to thank my family, the Lunch Squad and Dr J. M. Grebo, whose support has been unwavering over the years.

Finally, some credit is long overdue for Lady Ada Lovlace and Dr Grace Hopper, without whose groundbreaking work none of this would be possible.

Credits & About

This thesis was written in L^AT_EX, using latex templates made by Markus Billeter and Ludde Edgren.

Markus Billeter's template was originally created by Fredrik Warg, and updated by Martin Thuresson. The new, modified version of the template will be made available at

 <http://www.cse.chalmers.se/~billeter>

This document uses images from the “Silk Icons Set 1.3” by Mark James. The icons are licensed under a Creative Commons Attribution 2.5 License, and available at

 <http://www.famfamfam.com/lab/icons/silk/>.

The document also uses “ccBeamer 0.1” by Sebastian Pipping, which is licensed under Creative Commons Attribution–ShareAlike 3.0.

In compliance with the Swedish Research Council's policy on Open Access, the whole thesis is licensed under the Creative Commons Attribution-ShareAlike 3.0 License. For details on the licenses, see page ii. To learn more about Open Access, go to

 <http://www.openaccess.se>

An up to date version of this thesis will be available on the author's homepage. To get the L^AT_EX source, please go to

 <https://gitorious.org/skyman-s-licensiate-thesis>

Long live ☺!

:wq

¹and on other topics, ranging from pens to alectro dynamics, on the topic of which the Royal Blenheim pub in Oxford deserves a special mention...

Table of contents

I Summary

| | |
|---|-----------|
| 1 Introduction | 1 |
| 1.1 Nuclear fusion | 1 |
| 1.2 Fusion plasmas | 3 |
| 1.2.1 The fourth state of matter | 3 |
| 1.2.2 Confinement – the “Tokamak” | 5 |
| 1.2.3 Stability and quality of the confined plasma | 7 |
| 1.3 Plasma impurities | 8 |
| 1.4 Transport processes | 9 |
| 2 Turbulent impurity transport | 11 |
| 2.1 TE and ITG mode turbulence | 11 |
| 2.2 Impurity transport | 13 |
| 3 Gyrokinetic simulations | 15 |
| 3.1 GENE | 15 |
| 3.2 Experiments in silico | 16 |
| 4 Summary of papers | 19 |
| 4.1 Fluid and gyrokinetic simulations of impurity transport at JET . | 19 |
| 4.2 Impurity transport in temperature gradient driven turbulence . . | 20 |
| 4.3 Particle transport in density gradient driven TE mode turbulence | 22 |
| Bibliography | 23 |
| II Appended Papers | 27 |
| Paper I – Fluid and gyrokinetic simulations of impurity transport at JET | 29 |
| Paper II – Impurity transport in temperature gradient driven turbulence | 31 |
| Paper III – Particle transport in density gradient driven TE mode turbulence | 33 |

Part I

Summary

1

Introduction

1.1 Nuclear fusion

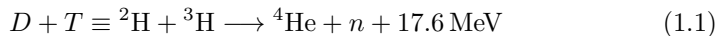
In a conventional nuclear power plant, the fuel consists of heavy elements whose nuclei split naturally, forming lighter atoms, in what is known as fission. Fusion, on the other hand, is the nuclear process where two lighter nuclei combine to form a heavier element. This does not happen naturally on Earth, but elsewhere in the universe it is commonplace: it is fusion that powers the stars. This was realised around the 1920s by Sir Arthur Eddington, and the dream of utilising this process for energy production was kindled at the same time [1].

Though fusion and fission power require very different operating scenarios, the fundamental principle that allows both fusion and fission to occur and release energy is the same. As can be seen in the curve in figure 1.1, the mass of an atom is not simply the sum of its nucleons – its neutrons and protons. This phenomenon is called the *mass defect*. [2] As neutrons and protons are added to or subtracted from an element, the combined mass is decreased if the product is closer to the minimum in the curve. The most common isotope of iron, ^{56}Fe , has been highlighted (\square) in the figure. As can be seen, iron is at the minimum of the mass curve, meaning that it is the element with the least mass per nucleon.

By Einstein's relation $E = mc^2$ [3] mass is a form of energy, wherefore the decrease in mass is also a decrease in energy, and generally, decreased energy means increased stability. The tendency of elements combining or falling apart to form more "iron like" elements is spontaneous, in the sense that it is statistically more likely to occur than the opposite. This can be understood from figure 1.1, by observing that in order to bring an element away from the minimum, mass in the form of energy has to be supplied from somewhere, whereas going toward ^{56}Fe the excess mass/energy need not fulfil any particular requirements – it has

a whole universe into which it can disperse. The conservation of energy – one of the most fundamental principles in all of Physics – demands that the missing mass be turned into other forms of energy, and it is this energy that is captured in nuclear power plants of both varieties. The typical fuel for fusion and fission are represented in figure 1.1 by the two highlighted isotopes ^2H and ^{238}U (Uranium) respectively. The ^2H is the isotope of Hydrogen called “heavy Hydrogen”, which is more commonly known as Deuterium and denoted D in fusion science. As can be seen, the energy that can potentially be gained by fusing light elements is many times greater per nucleon, and hence per kilogramme of fuel, than that which fission yields.¹ This is one of the reasons why fusion as a power source is so attractive.

That the fusion process is essentially spontaneous does not mean, however, that it is easy to accomplish. Whereas fission happens spontaneously on Earth, fusion requires much more exotic circumstances. In fission power plants, the nuclear process is mediated by neutrons, whereas for fusion to occur, the electrostatic repulsion between both the atoms’ negatively charged electron clouds, and then between the positively charged nuclei themselves, need to be overcome. Methods of accomplishing this normally require either extreme temperatures, extreme pressure, or a combination of the two. At sufficiently high temperature, collisions between atoms will be energetic enough to separate the electrons from the nuclei. If the frequency of recombining collisions is sufficiently low, a plasma is the result [5], meaning that it is easier to ionise a thin gas than a dense one. For fusion to occur, however, the resulting ions need to collide with enough force, that they break through the repulsive potential of the nuclear charges, which is many orders of magnitude higher than the repulsion from the electron clouds. The probability of a nuclear reaction to occur is quantified by the *cross section* for the reaction. The most favourable cross section for fusion is obtained for the fusion between Deuterium and Tritium (^3H) in the reaction [2, 5]:



where ^4He is an ordinary Helium ion, more often referred to as an α -particle, and n is a neutron. The total excess energy from the reaction in equation (1.1) is 17.6 MeV, distributed on the fusion products according to their mass, so that the total momentum is conserved, meaning that $\sim 4/5$ of the energy is deposited on the neutron. Because the neutron is uncharged, it is not confined by the magnetic fields used to contain the plasma, and will therefore leave the core region, depositing its energy in the wall of the plasma chamber, which is how energy will be extracted in a working power plant. The α -particles, on the other hand, will be caught in the magnetic field and, through collisions, deposit their excess energy to the fuel ions, heating the plasma. Efficient α -particle heating

¹ The scale in figure 1.1 is in eV, or *electron Volts*. $1 \text{ eV} \approx 1.6 \cdot 10^{-19} \text{ J}$, meaning that you would need roughly $2.5 \cdot 10^{19} \text{ eV}$ to heat 1g of water 1°C , but considering that Deuterium atoms are $\sim 1.5 \cdot 10^{26}$ to a kilo, there is still a lot of energy in one nuclear reaction [4].

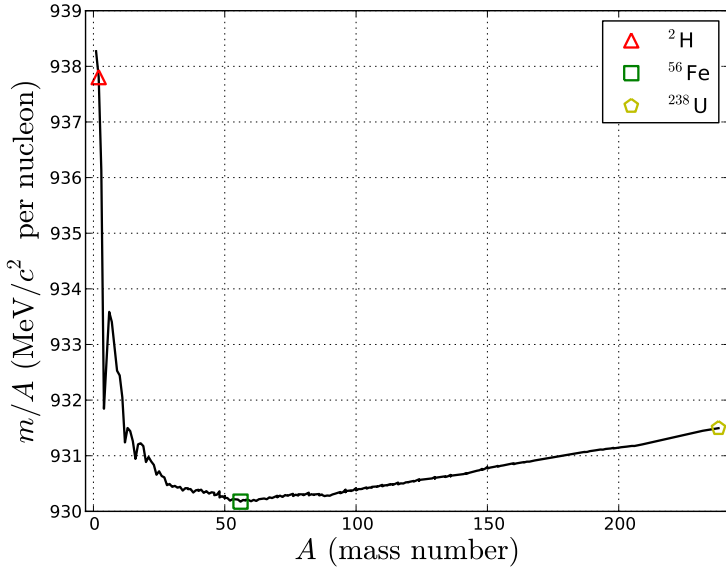


Figure 1.1: Mass defect for the stable nuclei. Deuterium (${}^2\text{H}$; \triangle) and Uranium (${}^{238}\text{U}$; \square) are indicated. Spontaneous fusion and fission moves towards the energy minimum (${}^{56}\text{Fe}$; \diamond). Based on data from [6] and [2].

therefore is the key to achieving self-sustained nuclear fusion. Unfortunately, Tritium is not a stable isotope of Hydrogen. It is radioactive with a half-life of 12.33 years, and so must be bred, for instance from Lithium [2, 4].

A striking example of fusion in Nature is the sun, which relies on the force of gravity to create the immense pressure needed for the fusion of protons and other elements to occur, which is the process that makes it and all other stars shine. The circumstances under which fusion can take place are very exotic from an Earthly stand-point, and very difficult to produce in a laboratory. Creating the conditions to allow for a high enough fusion cross section requires highly specialised devices and knowledge, which is why the engineering and science aspects of fusion research are both very important.

1.2 Fusion plasmas

1.2.1 The fourth state of matter

Super-heating or sufficiently depressurising a gas will eventually, through the processes outlined in section 1.1, lead to the separation of the electrons from the atoms in the material, resulting in an ionised gas – a plasma. In analogy with the solid, liquid and gaseous states of matter, plasmas are often referred to as

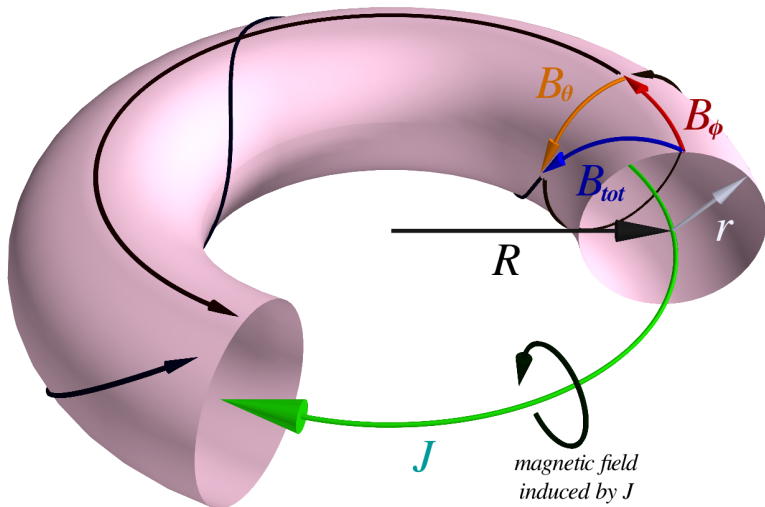


Figure 1.2: Illustration of the origin of the helical magnetic field lines in a tokamak. The toroidal (\mathbf{B}_ϕ ; ↶) and poloidal (\mathbf{B}_θ ; ↷) contributions to the total (\mathbf{B}_{tot} ; ↷) magnetic field are indicated. Neither \mathbf{B}_ϕ nor \mathbf{B}_θ exhibit the necessary twist, but their sum \mathbf{B}_{tot} is a magnetic field whose field lines spiral around the torus. The safety factor in the figure is $q \approx \frac{r}{R} \frac{B_\phi}{B_\theta} = 0.35$. The surfaces spanned by the field lines of \mathbf{B}_{tot} for different (minor) radii are referred to as flux surfaces. In most tokamaks their cross section is not fully circular. The poloidal magnetic field is induced by the plasma current (\mathbf{J} ; ↻) running along the toroidal axis of the plasma. Also indicated are the major (R ; →) and minor (r ; ↗) radii.

the *fourth state* of matter.

A more rigorous definition of a plasma is that

“[a] plasma is a quasineutral gas of charged and neutral particles which exhibits collective behaviour” [5],

where quasineutral means that the plasma is electrically neutral when viewed from a distance, but may exhibit charge fluctuations on small scales. In many ways a fluid,² plasmas are subject to the already complicated laws of fluid mechanics, but their behaviour becomes even more embroiled by the electromagnetic properties of the plasma, which introduce long range effects not present in

²in physics, the term *fluid* is used for both liquids and gasses, as opposed to solids

other media. These effects are what lead to collective behaviour in the plasma, and this property is the most important difference between a partly ionised gas and a proper plasma. The intermingling of these two areas of physics further implies, that acoustic and electromagnetic waves of all kinds coexist in the plasma, but often on very different time and length scales. This makes both analytical and numerical studies of the governing equations very challenging, if one wishes to capture the entirety of this intricate interplay.

Though exotic in many ways, plasmas exist in our everyday surroundings: in fluorescent tubes, neon signs and modern television sets. The kind of plasmas that occur naturally on Earth are rarer, but not uncommon. The Northern³ lights and lightning are perhaps the most well known examples. Fusion plasmas, however, need to be much hotter in order to have a high enough fusion cross section for fusion power to be feasible. In order to sustain a fusion grade plasma in a laboratory or a reactor, it needs to be separated from the surroundings; it needs to be confined.

In the sun and the stars, the confinement is accomplished by gravity, where the mass of the stellar body is enough to create the pressure needed for the fusion process to be self sustained. This is not, however, an option for earthbound plasmas.⁴ Instead, research into confining plasmas is divided into two main areas: magnetic and inertial confinement.

1.2.2 Confinement – the “Tokamak”

In the presence of a magnetic field, charged particles will experience a force perpendicular to their velocity and to the magnetic field. Because the force is always at a right angle to the velocity, it can not lead to an increase in the velocity of the particle, but only change its direction. This means that the particles will be confined to move in orbits around the magnetic field lines, but they remain free to move parallel to the field. In order to fully confine the particles, the parallel motion has to be restricted as well. This can be accomplished by increasing the magnetic field at the edges of the device, creating what is called a “magnetic mirror”. Though this will cause many particles to bounce back into the core of the plasma, it can be shown that particle losses at the ends of the device are unavoidable [5]. Therefore, most research into potential power plant designs have been devoted to the study of toroidal magnetic geometries – instead of tying off the ends of the magnetic field, the field lines are bent into a ring, closing on themselves. The toroidal configuration is illustrated in figure 1.2.

Since the ends are eliminated this way, so are the end losses, however, this setup comes with its own difficulties, stemming from the inhomogeneity of the magnetic field. For a simple toroidal magnetic field, it can be shown that, due to a combination of effects due to the gradient and curvature of the magnetic

³and, of course, Southern

⁴consider that Jupiter is in many ways a “failed” star: that the mass of the gas giant is too small to ignite its Hydrogen core illustrates the futility of gravitational confinement on Earth

field, the plasma will tend to be expelled from the core, toward the outside of the torus [5, 7]. This problem can be solved by introducing a twist (or “helicity”) in the magnetic field, so that the field lines – and the particles following them – spend time on both the in- and the outside of the device. In that way, the particles pushed toward the edge of the plasma when on one side of the torus, will be pushed back into the core when on the other side.

The twist is created by adding a field in the poloidal direction to the toroidal field; their sum will be a field with field lines spiralling around the torus. Figure 1.2 presents an illustration of how the helical field lines are generated. The first method of inducing this twist utilised external coils for both the poloidal and the toroidal magnetic fields. The devices were called “stellarators”, referring to the ambition of reproducing the workings of the sun and her stellar sisters here on Earth. Though stellarator research is a very active field (see e.g. [8, 9]), due to the difficulties of creating a favourable magnetic geometry by external means, most research since the sixties has shifted toward what is known as the “tokamak”,⁵ a configuration where the twist is accomplished by running a current through the core of the plasma. The rate of the helicity is measured by a parameter called the *safety factor* (q), which can be seen as the number of toroidal turns a magnetic field line make in one poloidal turn. It is directly proportional to the ratio of the toroidal magnetic field strength (B_ϕ) to the poloidal magnetic field strength (B_θ) [11], see figure 1.2.

In the tokamak design, instead of relying on external coils to create this twist, an axial current is induced in the plasma, creating the poloidal field through Ampere’s law [4]. This is done by treating the plasma – a very good conductor due to the free mobility of the electrons – as the secondary winding of a transformer, thus inducing a current in the plasma.⁶ The relationship between the plasma current and the helicity of the magnetic field lines is illustrated in figure 1.2.

A drawback of this method of introducing a helical twist in the magnetic field is that the electromagnetic field driving the plasma current is proportional to the change in the magnetic flux, as described by Faraday’s law of induction [4]. Therefore, the current can only be induced as long as the magnetic flux increases,

⁵There seems to be some confusion as to where the name “tokamak” came from, originally. Today, it is most often said to be an acronym for “*toroidalnaya kamera s magnitnaya katushka*”, which is Russian for “toroidal chamber with magnetic coils” [1]. In older works, however, one can instead read that it originates from “*toroidalnaya kamera s aksialnym magnitnym polem*”, or “toroidal chamber with axial magnetic field” [10]. While how and why the name came to shift its meaning remains a mystery, both acronyms are suitably descriptive of the device: the tokamak was developed in the Soviet Union in the middle of last century, and is indeed a toroidal chamber, with magnetic coils generating a magnetic field along the toroidal axis of the chamber. But this is common to all toroidal magnetic confinement devices, and so the name does not cut to the core of what sets the tokamak design apart from the others.

⁶this also helps to heat the plasma through resistive (or “ohmic”) heating, though at high temperatures the plasma is too good a conductor for this to be the only source of heating power

which it cannot do indefinitely. Eventually the transformer core will saturate, meaning that the plasma current can no longer be sustained. Though there are advanced operating scenarios under investigation that may circumvent this, tokamak operations are currently limited to pulsed mode. This is not a problem for the study of plasma dynamics, which usually involve time scales much shorter than the pulse time, but certainly a drawback when it comes to efficient power production.

1.2.3 Stability and quality of the confined plasma

Plasma confinement is a precarious process, only possible for precisely tuned parameters. One such parameter is the so called plasma β , which expresses the ratio of the particle pressure to the confining magnetic pressure. This parameter cannot supersede a few percent in tokamaks, or the plasma will be subject to large scale instabilities and disrupt, losing confinement almost at once [7, 11]. Pressure is related to the particle density and the temperature through the Boltzmann constant: $p = n_e k_B T$ [4].⁷ Therefore, an increase in either the number of particles or temperature would proportionally increase the pressure, eventually bringing it above the β -limit.

Though the β -limit constrains puts a severe constraint on the operating regimes available to achieve fusion power, it also makes the process inherently safe from anything like a nuclear melt-down. “Disruption” and “loss of confinement” may sound dire enough, considering that the temperature of the plasma can reach in excess of a hundred million degrees Celsius. The actual energy content of the plasma, however, is very modest, which can also be seen from the definition of pressure. Dimensionally, pressure is a measure of the energy density in a fluid. For a typical fusion plasma in ITER [12], the particle density will be $n_e \approx 10^{20} \text{ m}^{-3}$ for a volume of $V \approx 10^3 \text{ m}^3$, and the temperature will be roughly $T \approx 10^8 \text{ K}$. With $k_B \approx 10^{-23} \text{ J/K}$, combining these gives an energy density of approximately 10^5 J/m^3 . This is equivalent to 10^3 kPa , which is of the same order as the normal atmospheric pressure at sea level.⁸

Based on the energy content of the plasma, a measure of the quality of the confinement can be defined as the quotient of the energy content E and the power input P_{in} needed to sustain the plasma at that level of energy: $\tau_E \equiv E/P_{in}$, which has the dimension time. This is a measure of how quickly the energy would be lost, if power were not supplied, and is therefore called the *energy confinement time*. By dimensional arguments it can be shown that the power balance leads to a requirement for net energy production of $\tau_E n_e > (\tau_E n_e)_c$, for some critical value $(\tau_E n_e)_c$ [11]. This is called the *Lawson criterion*, and

⁷the subset $_e$ is for *electrons*, which is conventionally used, since the electron density in a fully ionised gas is a measure of the ion density, regardless of the number of different ion species

⁸the energy associated with the free electrons has been neglected here: the ionisation energy for Hydrogen is $\sim 10 \text{ eV}$, which translates to roughly 10^2 J/m^3 , so this contribution is negligible compared to the thermal energy of the ions

expresses the condition for power *break-even*. A more concrete performance parameter is that of the “fusion triple product”: $n_e T \tau_E > (n_e T \tau_E)_c$, valid in the temperature range considered for fusion. The triple product is a condition for a self sustained plasma, meaning that the necessary power to heat the plasma comes from the α particles generated by fusion events.⁹ In fusion experiments, the achieved triple product has been increasing exponentially over time since the dawn of fusion research, and the ITER device currently under construction is expected to continue this trend, with an estimated output power of five to ten times the input power [2, 7, 12]. Because of stability requirements, such as the β -limit mentioned above, the particle density and temperature are both restricted. Therefore, significantly increasing the Lawson parameter or the fusion triple product requires increasing the energy confinement time, which requires an understanding of the transport mechanisms at work.

1.3 Plasma impurities

Impurities – any ions that are not part of the fuel – tend to dilute the fuel, making collisions that produce fusion rarer, and thus reducing the fusion power. Heavier elements also tend to cool the plasma through radiative processes. Their high nuclear charge make them hard to ionise fully, even at the temperatures of a fusion plasma, and the electrons remaining bound to the impurity can then, rather than separate from the nucleus, respond to a collision by jumping to a higher electron orbit [13]. As the electrons relax, returning to the lower energy levels, they lose the energy gained in the collision, which is released in the form of photons. This is called *line radiation*, because the frequencies of the released photons correspond to lines in the light spectrum characteristic to the element that produced them. Since some heavy elements may never be fully ionised, line radiation can continue indefinitely. Therefore, even a small dilution of heavy impurities, can lead to significant energy losses in the plasma.

There are mainly three potential sources of impurities: the first being the walls of the reactor chamber. Due to the different roles played by different parts of the walls, they contribute both light and heavy impurities. The divertors, for instance, need to withstand the heavy power loads from energetic particles, and are therefore made of heavy metals such as Tungsten (W; nuclear charge $Z = 72$). Because of the danger of line radiation, using an element as heavy as Tungsten is not practical for all of the chamber, and hence lighter candidates with high heat resilience are used elsewhere. For example, at the Joint European Torus (JET, [14]) the new ITER-like wall project was recently initiated, testing the feasibility of using a coating of the light metal Beryllium (Be, nuclear charge $Z = 4$) on the plasma facing first wall of the reactor chamber [15].

⁹both the Lawson criterion and the fusion triple product are valid measures of the quality of fusion plasmas for magnetically as well as initially confined fusion plasmas, but in magnetic confinement fusion n_e is typically small and τ_e large, while the opposite holds for inertial confinement fusion

Not all impurities, however, are contaminants. The second main source of plasma impurities is injections of particles for control purposes. Here the cooling mechanisms are beneficial to the operation of the fusion reactor. By injecting elements such as Argon (Ar, $Z = 18$) that radiate energy in the right locations, the heat load on components such as the divertors can be spread out, protecting them from wearing out [16]. Impurities are also injected for experimental purposes, in order to study their transport properties.

Finally, the fuel ions will, in a working power plant, be diluted by the steady production of α -particles (sometimes referred to as “Helium ash”) through fusion reactions.

Of major concern is whether different kinds (or “species”) of impurities will experience an inward or an outward pinch. Simulations of this is the main topic in this thesis.

1.4 Transport processes

Understanding the transport of particles, heat, momentum etc. in fusion plasmas is a very important topic of research. As mentioned above, controlling the transport properties of the plasma may be the only way forward when it comes to increasing the fusion efficiency, as measured by the Lawson parameter and the fusion triple product (section 1.2.3).

In fluids, it is common to describe the transport as consisting of diffusion and convection.¹⁰ Diffusion is the (seemingly) random spreading of a quantity in a fluid. It can often be understood as being mediated by collisions in the flow leading to a dispersive random walk [17]. Diffusive transport is driven by gradients, and so diffusion is directed from areas of abundance, to areas of scarcity. Thereby diffusion tends to even out profiles of temperature, density etc.

The convective part of the transport relates to bulk motion of particles in a fluid. It can either be up or down gradient, depending on the situation. In fusion plasmas, a net convective velocity is often referred to as a “pinch”.

Transport is often separated into *classical* and *anomalous* transport, where classical refers to transport dominated by collisions, whereas all other observed transport is termed anomalous [18]. Experiments have shown that, for most regions of the fusion plasma, anomalous transport clearly dominates over classical transport [18]. The most common example of anomalous transport in plasmas is turbulent transport. Turbulence is often associated with strong gradients, which represent free energy within a system that can drive instabilities. It is difficult to envision any classical situation, where the gradients are more pronounced than in a modern magnetic confinement fusion device, however, turbulence is a very common phenomenon in all of Nature. Hence it has been a topic of study for

¹⁰advection is often used in place of convection, using convection to mean the sum of advective and diffusive transport

scientists and engineers for the better part of three hundred years, but its nonlinear character means that studying the effects of turbulence is very challenging. One main feature of turbulence is the interaction and interchange between different time and length scales, meaning that turbulent transport cannot be properly described by simple convection and diffusion. Locally, however, this approximation can be valid, when looking at space and time averaged fluxes [19–22]. The turbulent transport then manifests itself as effective diffusivities and pinches, at different minor radii.

All turbulent dynamics exhibit nonlinearities, making exact analytical solutions to equations of motion hard to come by, necessitating the application of numerical methods. To aid researchers when predicting and interpreting experimental outcomes, numerical tools have been developed to study the transport. Both dedicated transport solvers and more general plasma codes are used to this end, and one main topic in this thesis is comparing results from two such models: a multi-fluid and a gyrokinetic model.

2

Turbulent impurity transport

2.1 TE and ITG mode turbulence

The turbulence in magnetically confined fusion plasmas, such as those in Tokamaks like the proposed ITER device [12], has important and non-trivial effects on e.g. the quality of the energy confinement – effects that are hard to tackle both analytically and numerically. The problem of transport of energy and particles in a Tokamak plasma is an area of research where turbulence plays a major role, and that is intimately associated with the performance of future fusion reactors.

Many types of instabilities that exhibit this behaviour can be explained as analogous to the Rayleigh–Taylor instability, where a dense fluid is supported by a less dense fluid against the influence of gravity [5, 7, 11]. This is the case on the outboard side of the tokamak, which for its propensity for driving instabilities is called the *bad curvature region*. The profiles of the density and temperature perturbations will therefore have maxima on the outside, and minima on the inside, which is called *ballooning* [7, 23].

The origin of turbulent transport in tokamak plasmas is the fluctuations in the electric and magnetic fields. Crucially, the magnitude of the transport does not only depend on the the magnitude of the fluctuation, but also on the extent of the phase correlation between the fluctuating quantities. For instance, for a net particle flux, the fluctuation in the velocity field needs to be accompanied by a fluctuation in the particle density that is correlated with the velocity fluctuation.

For the linear modes driving the turbulence considered in this thesis – ion temperature gradient (ITG) and trapped electron (TE) modes in low β plasmas – the perturbation can be considered to be mainly electrostatic. Both the ITG and the TE mode are examples of so called reactive drift wave modes. They are both

associated with length scales known to cause transport ($k_\theta \rho_s \approx 0.3$), and their mode frequencies are of the same order as the magnetic and diamagnetic drift frequencies ($\omega_r \sim \omega_D, \omega_*$).

The ITG mode can be understood as arising from a fluctuation in the temperature distribution, which under the influence of the poloidal magnetic drift causes a response in the ion density. If the electrons are considered adiabatic, they will respond by quickly redistributing according to the new landscape, creating an electric potential difference between the compressible ions, and the thermal electrons. The resulting electric field (\mathbf{E}) will, in turn, lead to a drift velocity perpendicular to \mathbf{E} and to the magnetic field (\mathbf{B}) – the $\mathbf{E} \times \mathbf{B}$ drift – acting on the temperature perturbation, and thus closing the feedback loop. In the bad curvature region, this feedback will be positive leading to an instability. The origin of the TE mode instability is similar in nature to the origin of the ITG mode [7].

In the case of a purely electrostatic perturbation, the particle flux of ion species j can formally be written [18]:

$$\Gamma_j = \langle \delta n_j v_E \rangle, \quad (2.1)$$

where δn_j is the perturbation in the density of species j and v_E is the $\mathbf{E} \times \mathbf{B}$ drift velocity [7]. The angled brackets imply a time and space average over all unstable modes.

Deriving expressions for the drift velocities and the density response etc. can be done using different theoretical frameworks. In kinetic theory the plasma is described through distribution functions of velocity and position for each of the included plasma species. Hence, kinetic equations are inherently six-dimensional, however, in magnetically confined fusion plasmas the confined particles are generally constrained to tight orbits along field lines. This motivates performing an average over the gyration, reducing the problem to five-dimensional gyrokinetic equations [24–27]. Since the equations governing the evolution of the distributions are all coupled, the resulting decrease in numerical complexity is considerable. Fluid theory, on the other hand, is derived by taking the moments of the kinetic equations to some order, making them tractable by finding an appropriate closure [7]. In addition to making the workings of the plasma more accessible, by reintroducing familiar physical concepts such as pressure and density, fluid models are also several orders of magnitude more computationally efficient.

Whether δn_j and v_E are derived from fluid or gyrokinetic theory, performing the average in equation (2.1) for a fixed length scale $k_\theta \rho_s$ of the turbulence, leads to an expression of the following form:

$$\frac{R\Gamma_j}{n_j} = D_j \frac{R}{L_{n_j}} + D_{T_j} \frac{R}{L_{T_j}} + R V_{p,j}. \quad (2.2)$$

The first term in equation (2.2) corresponds to diffusion, the second to the thermodiffusion and the third to the convective velocity (pinch), where $R/L_{X_j} = -R\nabla X_j/X_j$, with $X = n, T$, are the normalised logarithmic gradients of density and temperature for species j , and R is the major radius of the tokamak. The pinch here contains contributions from curvature and parallel compression effects, however, the thermodiffusive term in equation (2.2) is sometimes referred to as the thermopinch and included in the convective velocity, so as not to confuse it with the proper (i.e. density gradient driven) diffusion. These terms have been described in detail in previous work, see e.g. [19–21] and Paper I and Paper II in this thesis.

2.2 Impurity transport

For trace impurities, equation (2.2) can be uniquely written as a linear function of ∇n_Z , offset by a convective velocity or “pinch” V_Z :

$$\Gamma_Z = -D_Z \nabla n_Z + n_Z V_Z \Leftrightarrow \frac{R\Gamma_Z}{n_Z} = D_Z \frac{R}{L_{n_Z}} + R V_Z, \quad (2.3)$$

where D_Z is the impurity diffusion coefficient, and V_Z is the impurity convective velocity with the thermopinch included. Both the D_Z and V_Z are independent of ∇n_Z in the trace impurity limit [19]. Z refers to the charge number of the impurity.

In the core of a steady-state plasma with fuelling from the edge (i.e. no internal particle sinks or sources), the impurity flux Γ_Z will go to zero. The zero-flux impurity density gradient (peaking factor) is defined as

$$PF_Z = -\frac{R V_Z}{D_Z}, \quad (2.4)$$

for the value of the impurity density gradient that gives zero impurity flux.¹ Solving the linearised equation (2.3) for R/L_{n_Z} with $\Gamma_Z = 0$ yields the interpretation of PF_Z as the gradient of zero impurity flux, and it quantifies the balance between convective and diffusive impurity transport. Specifically, the sign of the peaking factor is determined by the sign of the pinch, meaning that $PF > 0$ is indicative of a net inward impurity pinch, giving a peaked impurity profile. Conversely, if $PF < 0$ the net impurity pinch is outward, leading to a hollow impurity profile. The latter condition is called a *flux reversal*, and conditions leading to this are of particular interest, since an accumulation of impurities in the core of the plasma is preferably to be avoided (see section 1.3). The relationship of PF to D_Z and V_Z is illustrated in figure 3.3.

Much of the observed difference between the TE and ITG mode dominated cases – a major topic in the appended articles – can be understood from the convective

¹this number is also sometimes referred to the *Péclet number* [28, 29]

velocity V_Z in equation (2.3). Particularly, the pinch contains two terms that depend on the impurity charge number Z [19]:

- thermodiffusion (thermopinch):

$$- V_{\nabla T_Z} \sim \frac{1}{Z} \frac{R}{L_{T_Z}},$$

- inward for TE mode ($V_{\nabla T_Z} < 0$), outward for ITG mode ($V_{\nabla T_Z} > 0$),

- parallel impurity compression:

$$- V_{\parallel, Z} \sim \frac{Z}{A_Z} k_{\parallel}^2 \sim \frac{Z}{A_Z q^2} \approx \frac{1}{2q^2},$$

- outward for TE mode ($V_{\parallel Z} > 0$), inward for ITG mode ($V_{\parallel Z} < 0$).

Here $1/k_{\parallel}$ decides the wavelength of the parallel structure of the turbulence. Due to the ballooning character of the modes considered, this is proportional to the safety factor (q). The Z dependence in the parallel impurity compression is expected to be weak, since the mass number is approximately $A_Z \approx 2Z$ for an impurity species with charge Z . The thermodiffusive contribution, however, can dominate the transport for low Z impurities (such as the Helium ash). The direction of these contributions to the pinch are governed mainly by the considered mode's drift direction, which is different for TE and ITG modes [7].

3

Gyrokinetic simulations

3.1 GENE

The GENE code [30–33] is a massively parallel gyrokinetic Vlasov code, solving the nonlinear time evolution of the gyrokinetic distribution functions on a fixed grid in phase space. The gyrokinetic equations are derived from the kinetic equations by performing an average of the particles' gyrations around the field lines, so that the equations follow the centre of gyration, rather than the explicit orbits. This reduces the velocity space coordinates from three to two directions: parallel velocity and magnetic moment. Following the conventions of GENE, these are represented by v and μ respectively. In real space, the radial (x) and bi-normal (y) dependencies are treated spectrally, i.e. those directions are discretised explicitly in k -space, whereas the toroidal (z) direction is discretised in real space. Because all phase space coordinates are coupled nonlinearly, the decrease from six to five phase space coordinates means a significant increase in computational efficiency.

There are some requirements that need to be fulfilled, for this simplification of the equations to be appropriate. First of all, the Larmor gyro-radii (ρ) of the plasma species have to be small, and the associated cyclotron frequencies (Ω) large, compared to the system size ($\sim R$) and frequency (ω) of the turbulent fluctuations respectively; secondly, the fast motion of the particles along the field lines lead to the requirement that the typical wave length of the parallel structure of the turbulence ($1/k_{\parallel}$) is much longer than the perpendicular ditto ($1/k_{\perp}$); and third, the energy associated with turbulent fluctuations need to be small compared to the thermal background energy. This is called the gyrokinetic ordering, which generally holds for tokamak plasmas [25, 31]. Formally, this can be written:

$$\frac{\rho}{R} \sim \frac{\omega}{\Omega} \sim \frac{k_{\parallel}}{k_{\perp}} \sim \frac{q\phi}{T} \ll 1. \quad (3.1)$$

3.2 Experiments in silico

In this work, GENE simulations were performed in a flux tube geometry with periodic boundary conditions in the perpendicular directions. The flux tube is in essence a box that is elongated and twisted along with the \mathbf{B} field as the field lines traverse the tokamak. Its application relies on the assumption that the scales of the phenomena of interest are all small compared to the size of the flux tube. The periodic boundary conditions also imply the assumption, that local effects dominate over global. This is generally true in the core of the plasma.

The instantaneous memory usage of a nonlinear GENE simulation is often of the order of several gigabyte. This means that even conservatively saving runtime data is unfeasible. Instead, GENE reduces the raw field data to physically comprehensible fields, which are saved to disk at intervals specified by the user. An example of this is shown in figure 3.1, where a cross section of the simulation domain is shown. The highlighted area corresponds to a cross section of the flux tube, whereas the rest of the annulus is approximated from the whole three dimensional data set. The quantity shown is the fluctuations in the electrostatic potential ϕ near the end of a TE mode simulation. The saved data can be loaded into e.g. GENE’s native diagnostics tool, and after further refinement, data for specific physical quantities can be extracted.

Images such as the one presented in figure 3.1 are useful for providing a quick “sanity checks” for the simulations:

- Are the turbulent features sufficiently small, compared to the domain size?
- Are they large enough, compared to the resolution?
- Are there features that look artificial?

Beyond that, however, the derived data is still difficult to compare directly with experiments – numerical and physical alike – before it has been further distilled. By performing different averages over the simulation domain, scalar quantities are derived, such as mean fluctuation levels of particle densities and of the electrostatic potential, and integrated particle and heat fluxes across the flux tube boundaries. Since such scalar quantities are often what is needed for further analysis, GENE by default calculates and saves a number of such averages at regular intervals. Because they are scalars rather than fields, the resulting time series can afford a very good temporal resolution, without hampering simulation performance or running out of disk space. Two such time series are presented in figure 3.2. They show the space averaged fluctuations in background ion density (n_H^2) and impurity flux (Γ_Z) for the same simulation as in figure 3.1.

In order to reach the quantities of principal interest in this study, however, the data needs to be even further condensed. First, a time average is performed on time series of the impurity flux in order to obtain a mean flux ($\langle \Gamma_Z \rangle$), as illustrated in 3.2. This average is performed for simulations with at least three

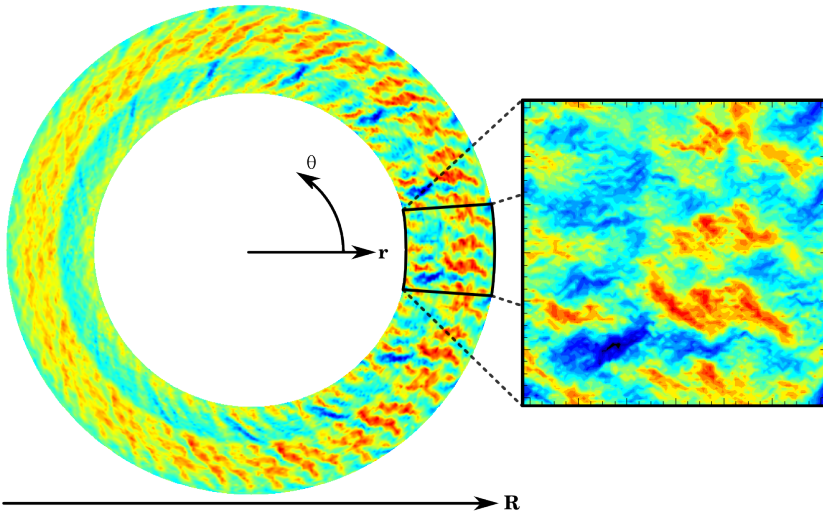


Figure 3.1: A cut from the toroidal annulus made up of the flux tube as it twists around the torus following the B field; see figure 1.2. Shown are the fluctuations in the electrostatic potential (ϕ). A cross-section of the flux tube with the side $\sim 125 \rho$ is indicated. Data from NL GENE simulation of TE mode turbulence at $t \approx 300 R/c_s$; parameters as in figure 4.1a.

different values for the impurity density gradient ($-R\nabla n_Z/n_Z = R/L_{n_Z}$). As is illustrated in figure 3.3, the linearised impurity flux equation (2.3) is then fitted to the obtained average fluxes. The quotient of the obtained diffusion coefficient (D_Z) and convective velocity (V_Z) then yields the peaking factor (PF), which quantifies the balance of diffusive and convective transport for the impurity species (see section 2.2 for details).

Finally, PF is calculated for several different values of e.g. the impurity charge (Z) in order to obtain a scaling, which can be compared to experiments and other models. Such a scaling is presented in figure 4.1a, where the sample followed in the figures mentioned previously has been highlighted (\circ).

In the process of generating a scaling such as the nonlinear scaling in figure 4.1a, the equivalent of several terabyte of instantaneous data is distilled into just a couple of floating point numbers – a remarkable compression rate, to say the least. GENE can also be run in quasilinear mode, a method that is considerably less demanding when it comes computer resources since the non-linear coupling between length scales is ignored [32–34]. The method is only used to study one mode at a time, and only for the particular length scale $k_\theta \rho_s$ of choice. If the length scale is chosen appropriately, however, the quasilinear simulation will capture the essential features of the dynamics, and it is useful for getting a qualitative understanding of the physical processes. As used in this work, it captures the contribution from the most unstable mode, not from any sub-dominant modes. The methodology is the same as for the nonlinear simulations.

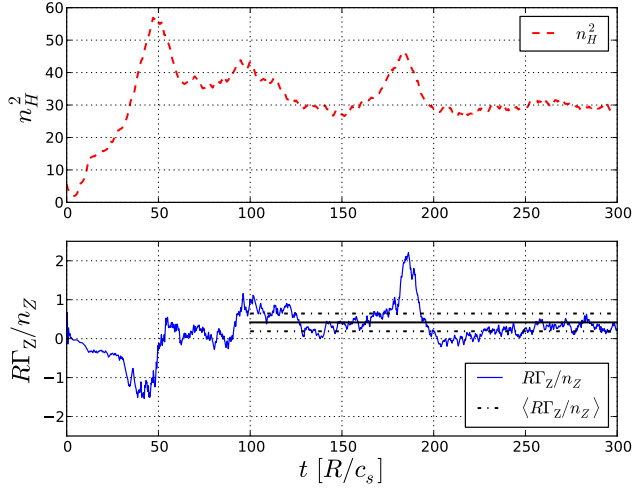


Figure 3.2: Time series showing fluctuations in the main ion density (n_H^2) and impurity flux (Γ_Z) after averaging over the whole flux tube; see figure 3.1. The average impurity flux ($\langle \Gamma_Z \rangle$) is calculated from Γ_Z , discarding the first portion so as not to include the linear phase of the simulation. $\langle \Gamma_Z \rangle$ is used for finding the peaking factor for the impurity species; see figure 3.3. NL GENE simulation with He impurities; parameters as in figure 4.1a, with $R/L_{n_Z} = 1.5$. An estimated uncertainty of one standard error is indicated.

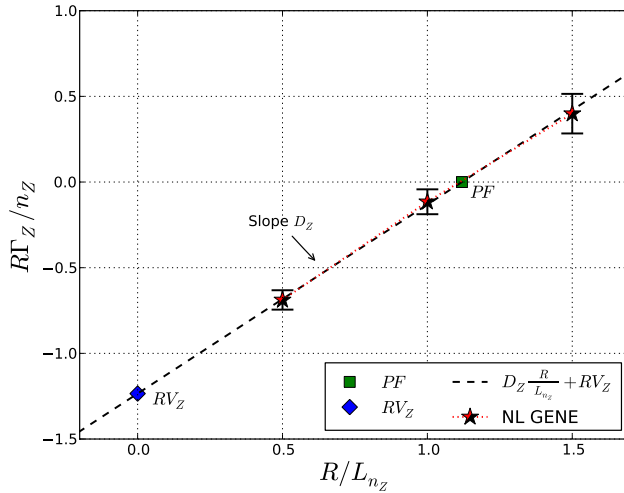


Figure 3.3: Impurity flux (Γ_Z) dependence on the impurity density gradient (R/L_{n_Z}), illustrating the peaking factor (PF), the diffusivity (D_Z) and pinch (V_Z), and the validity of the linearity assumption of equation (2.3) for trace impurities. Γ_Z is acquired as a time average of the impurity flux; see figure 3.2. D_Z and V_Z are calculated from the data, taking the estimated uncertainty into account. NL GENE simulations with He impurities; parameters as in figure 4.1a. An estimated uncertainty of one standard error is indicated.

4

Summary of papers

4.1 Fluid and gyrokinetic simulations of impurity transport at JET

Paper I deals with impurity transport due to ion temperature gradient (ITG) mode dominated turbulence in the core plasma region of dedicated impurity injection experiments #67730 and #67732 at JET. The main results are comparisons between experimental results and results from nonlinear and quasilinear gyrokinetic and nonlinear fluid simulations for the impurity peaking factor (see section 2.2) in the form of scalings of the peaking factor (PF) with the impurity charge number Z . The simulations were performed both with one impurity species alone, and with impurities along with 2% C background, which is the common scenario at JET.

A good qualitative agreement between the experimental impurity peaking and both models was obtained, except for Carbon impurities, where the flat or hollow profiles observed in experiments were not reproduced by the numerical simulations. It was observed that the peaking factor increased rapidly for low impurity charge, reaching a saturation for higher values of Z with $2 \lesssim PF \lesssim 3$, which is much lower than neoclassical predictions. Further, the effects of increasing the charge fraction of impurities, of collisions, and of $\mathbf{E} \times \mathbf{B}$ shearing on the impurity peaking were investigated. All three resulted in lowered peaking factors for the low Z impurities. Scalings with the ion temperature gradient for different species of impurities were also obtained, and also here a good qualitative agreement between the models was observed, though the nonlinear gyrokinetic simulations predicted substantially higher fluctuation levels than the fluid model.

The article was published in Plasma Physics and Controlled Fusion in October 2011 (vol. 53, no. 10, p. 105005–18).

4.2 Impurity transport in temperature gradient driven turbulence

Rather than comparing with experiments, as in [Paper I](#), the main focus in [Paper II](#) is the comparison of numerical models: nonlinear and quasilinear gyrokinetics, and a computationally efficient nonlinear multi-fluid model. The secondary focus is the comparison of temperature gradient driven TE mode scalings of the impurity peaking factor, with results for the ITG mode similar to those studied in [Paper I](#).

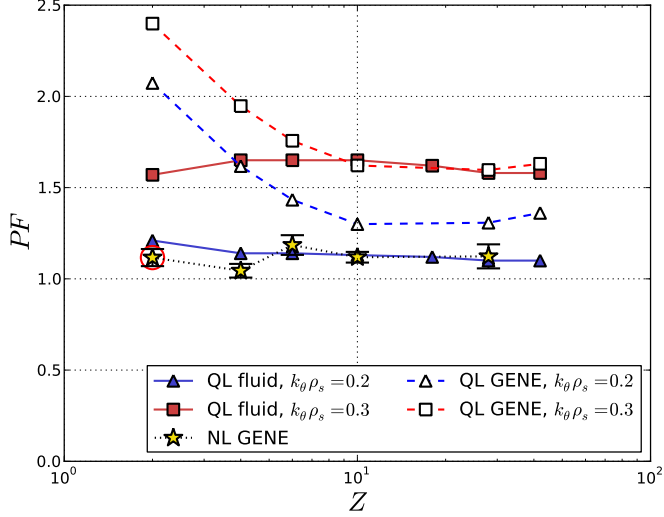
Scalings of the impurity peaking factor with the impurity charge number, and with the background temperature and density gradients ($R/L_{T_{i,e}}$ and R/L_{n_e}) were obtained for both modes of turbulence. Nonlinear gyrokinetic scalings with Z and R/L_{T_e} were obtained for the TE mode dominated case.

A falling trend of PF observed for increasing Z in the TE mode case was observed, whereas for the ITG mode the same trend as in [Paper I](#) was seen, with the peaking factor saturating at higher values of Z for both modes. This is illustrated in [figure 4.1](#). A theoretical explanation for this difference was found from the signs and Z dependence of the thermodiffusive contribution to the impurity convective velocity.

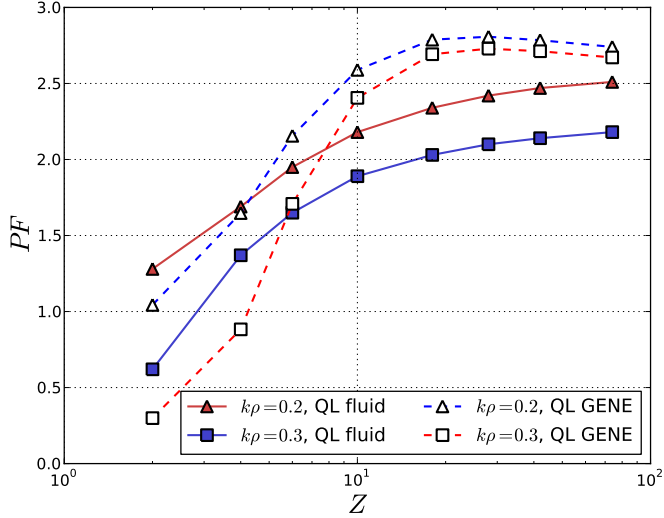
For all the scalings, the results show a good qualitative agreement between the models. The quasilinear gyrokinetic simulations were observed to overestimate the peaking factor, compared to the nonlinear results. The fluid results were, however, shown to be sensitive to the choice of the parallel mode structure assumed in the simulations, which may hint at an avenue of improvement for the fluid model.

The impurity peaking factor was also compared to the main ion peaking factor as calculated from fluid simulations. The main ion peaking was found to be slightly larger than the corresponding impurity peaking factors.

The work included in this paper builds in part on results presented at the *EPS*, *PDC*, and *RUSA* conferences in 2010; see [page vi](#). The article has been submitted to *Physics of Plasmas*.



(a) dependence of the peaking factor (PF) on Z for the TE case



(b) dependence of the peaking factor (PF) on Z for the ITG case

Figure 4.1: Scalings of the peaking factor (PF) with impurity charge (Z). Parameters are $q = 1.4$, $s = 0.8$, $\epsilon = r/R = 0.143$ in both subfigures, with $R/L_{T_i} = R/L_{T_Z} = 3.0$, $R/L_{T_e} = 7.0$, $R/L_{n_e} = 2.0$ for the TE case (figure 4.1a), and $R/L_{T_i} = R/L_{T_Z} = 7.0$, $R/L_{T_e} = 3.0$, $R/L_{n_e} = 3.0$ for the ITG case (figure 4.1b). The error bars for the NL GENE results in figure 4.1a indicate an estimated error of one standard deviation. The sample for the He impurity acquired from the data illustrated in figure 3.3 and figure 3.2 is highlighted (\circ).

4.3 Particle transport in density gradient driven TE mode turbulence

The work in [Paper III](#) complements the work in [Paper II](#) by investigating impurity transport in TE mode turbulence driven by steep background density gradients, as relevant to H-mode physics.

Main ion and impurity transport were both examined, and scalings with Z and R/L_{n_e} obtained from a quasi- and nonlinear gyrokinetic model were compared with results from the fluid model. The scaling with impurity charge was observed to be weak for the parameters considered, and the peaking factor was shown to saturate at values significantly smaller than the driving electron gradient in the steep electron gradient regime. Good qualitative agreements between the models were obtained, and it was observed that, for the TE mode, the quasilinear gyrokinetic simulations usually overestimated PF , whereas the fluid results underestimated it, compared to the nonlinear gyrokinetic results.

The work included in this paper was presented at the *13th International Workshop on H-mode Physics and Transport Barriers* in 2011; see [page vi](#). The article has been submitted to the Nuclear Fusion special issue for the above mentioned workshop.

Bibliography

- [1] J. Wesson. *The Science of JET*. JET Joint Undertaking, 2000. URL <http://www.iop.org/Jet/fulltext/JETR99013.pdf>.
- [2] K. S. Krane. *Introductory Nuclear Physics*. John Wiley & Sons, Inc., 1988.
- [3] A. Einstein. Ist die Trägheit eines Körpers von seinem Energieinhalt abhängig? *Annalen der Physik*, 323(13):639–641, 1905.
- [4] C. Nordling and J. Österman. *Physics Handbook*. Studentlitteratur, 6th edition, 1999. “Physics”.
- [5] F. F. Chen. *Introduction to Plasma Physics and Controlled Fusion*, volume Volume 1: Plasma Physics. Plenum Press, 2nd edition, 1984.
- [6] M. Pössel. Is the whole the sum of its parts? *Einstein Online*, 4:1003, 2010.
- [7] J. Weiland. *Collective Modes in Inhomogeneous Plasmas*. IoP Publishing, 2000.
- [8] Large Helical Device (LHD). URL <http://www.lhd.nifs.ac.jp/en/>.
- [9] Wendelstein 7-X (W7-X). URL <http://www.ipp.mpg.de/ippcms/eng/for/projekte/w7x/>.
- [10] “tokamak”, Merriam-Webster.com, 2011. Merriam-Webster, Inc. URL <http://www.merriam-webster.com/dictionary/tokamak>. (Dec. 17, 2011).
- [11] R. D. Hazeltine and J. D. Meiss. *Plasma Confinement*. Dover Publications, 2003.
- [12] ITER¹. URL <http://www.iter.org/>.
- [13] C. S. Harte, C. Suzuki, and T. Kato, et al. Tungsten spectra recorded at the LHD and comparison with calculations. *J. Phys. B*, 43(20):205004, 2010.

¹formerly “International Thermonuclear Experimental Reactor”

- [14] Joint European Torus (JET). URL <http://www.efda.org/jet/>.
- [15] G. F. Matthews, P. Edwards, H. Greuner, A. Loving, and H. Maier et al. Current status of the JET ITER-like Wall Project. *Phys. Scr.*, 2009 (T138):014030, 2009.
- [16] A. Loarte, J. W. Hughes, M. L. Reinke, J. L. Terry, and B. LaBombard et al. High confinement/high radiated power H-mode experiments in Alcator C-Mod and consequences for International Thermonuclear Experimental Reactor (ITER) $Q_{DT} = 10$ operation. *Phys. Plasmas*, 18(5):056105, 2011.
- [17] A. Einstein. Über die von der molekularkinetischen Theorie der Wärme geforderte Bewegung von in ruhenden Flüssigkeiten suspendierten Teilchen. *Annalen der Physik*, 323(8):549–560, 1905.
- [18] P. C. Liewer. Measurements of microturbulence in tokamaks and comparisons with theories of turbulence and anomalous transport. *Nucl. Fusion*, 25(5):543, 1985.
- [19] C. Angioni and A. G. Peeters. Direction of impurity pinch and auxiliary heating in tokamak plasmas. *Phys. Rev. Lett.*, 96:095003, 2006.
- [20] H. Nordman, T. Fülöp, J. Candy, P. Strand, and J. Weiland. Influence of magnetic shear on impurity transport. *Phys. Plasmas*, 14(5):052303, 2007.
- [21] H. Nordman, R. Singh, and T. Fülöp et al. Influence of the radio frequency ponderomotive force on anomalous impurity transport in tokamaks. *Phys. Plasmas*, 15:042316, 2008.
- [22] H. Nordman, A. Skyman, P. Strand, C. Giroud, F. Jenko, and F. Merz et al. Fluid and gyrokinetic simulations of impurity transport at JET. *Plasma Phys. Contr. F.*, 53(10):105005, 2011.
- [23] A. Hirose, L. Zhang, and E. Elia. Higher order collisionless ballooning mode in tokamaks. *Phys. Rev. Lett.*, 72(25):3993, 1994.
- [24] T. M. Antonsen and B. Lane. Kinetic equations for low frequency instabilities in inhomogeneous plasmas. *Phys. Fluids*, 23(6):1205, 1980.
- [25] E. A. Frieman and L. Chen. Nonlinear gyrokinetic equations for low-frequency electromagnetic waves in general plasma equilibria. *Phys. Fluids*, 25(3):502, 1982.
- [26] T. S. Hahm, W. W. Lee, and A. Brizard. Nonlinear gyrokinetic theory for finite-beta plasmas. *Phys. Fluids*, 31(7):1940, 1988.
- [27] A. Brizard. Nonlinear gyrokinetic Maxwell-Vlasov equations using magnetic co-ordinates. *J. Plasma Phys.*, 41(3):541, 1989.

- [28] W. Arter. Numerical simulation of magnetic fusion plasmas. *Rep. Prog. Phys.*, 58(1):1, 1995.
- [29] O. G. Bakunin. Scaling law and fractality concepts in models of turbulent diffusion. *Plasma Phys. Contr. F.*, 45(10):1909, 2003.
- [30] The GENE code. URL <http://www.ipp.mpg.de/~fsj/gene/>.
- [31] F. Jenko and W. Dorland. Nonlinear electromagnetic gyrokinetic simulations of tokamak plasmas. *Plasma Phys. Contr. F.*, 43(12A):A141, 2001.
- [32] T. Dannert. *Gyrokinetische Simulation von Plasmaturbulenz mit gefangenen Teilchen und elektromagnetischen Effekten*. Ph.d. thesis (monography), Technischen Universität München, 2005.
- [33] F. Merz. *Gyrokinetic Simulation of Multimode Plasma Turbulence*. Ph.d. thesis (monography), Westfälischen Wilhelms-Universität Münster, 2008.
- [34] T. Dannert and F. Jenko. Gyrokinetic simulation of collisionless trapped-electron mode turbulence. *Phys. Plasmas*, 12(7):072309, 2005.

Part II

Appended Papers

Fluid and gyrokinetic simulations of impurity transport at JET

H. Nordman, **A. Skyman**, P. Strand, C. Giroud, F. Jenko, F. Merz, V. Naulin, T. Tala and the JET–EFDA Contributors

Postprint, see DOI link for the published version

Plasma Physics and Controlled Fusion
vol. 53, no. 10, p. 105005–18

 [doi:10.1088/0741-3335/53/10/105005](https://doi.org/10.1088/0741-3335/53/10/105005)

 <https://publications.lib.chalmers.se/cpl/record/index.xsql?pubid=147198>

**Impurity transport in temperature gradient driven
turbulence**

A. Skyman, H. Nordman, P. Strand

Preprint

Physics of Plasmas
(submitted)

**Particle transport in density gradient driven
TE mode turbulence**

A. Skyman, H. Nordman, P. I. Strand

Presented at the
13th International Workshop on H-mode Physics and Transport Barriers
Oxford, UK, October 2011

Preprint

Nuclear Fusion SPE 2012
(submitted)

